A Galactolipid Possesses Novel Cancer Chemopreventive Effects by Suppressing Inflammatory Mediators and Mouse B16 Melanoma

Chia-Chung Hou,[1] Yi-Ping Chen,[1] Jyh-Horng Wu,[2] Chi-Chang Huang,[1] Sheng-Yang Wang,[2] Ning-Sun Yang,[1] and Lie-Fen Shyur[1]

[1]Agricultural Biotechnology Research Center, Academia Sinica, Taipei, Taiwan, Republic of China and
[2]Department of Forestry, National Chung-Hsing University, Taichung, Taiwan, Republic of China

Abstract

Crassocephalum rabens **(Asteraceae) is a popular anti-inflammatory folk medicine and food supplement. We investigated the cancer chemopreventive bioactivity of *C. rabens* phytocompounds *in vitro* and *in vivo* using cell- and gene-based bioassays and a mouse B16 melanoma model. The bioactive glyceroglycolipid 1,2-di-*O*-α-linolenoyl-3-*O*-β-galactopyranosyl-*sn*-glycerol (dLGG) that was identified from *C. rabens* was found *in vitro* and *in vivo* to be a potent nitric oxide (NO) scavenger. dLGG treatment inhibited both mRNA and protein expression of inducible NO synthase and cyclooxygenase-2 (COX-2) in murine macrophages and inhibited *COX-2* gene transcription in 12-*O*-tetradecanoylphorbol-13-acetate (TPA)–treated B16 cells. In immunohistochemical studies, dLGG inhibited TPA-induced expression of COX-2 and nitration of proteins in mouse skin. dLGG could also significantly inhibit lipopolysaccharide-induced prostaglandin E_2 production in murine macrophages. Furthermore, dLGG prevented nuclear translocation of cytoplasmic nuclear factor-κB (NF-κB) by suppressing IκBα phosphorylation and degradation. Structure-activity relationship study by electrophoretic mobility shift assay indicated that the dilinolenoylglycerol moiety in dLGG is the essential structural feature preventing NF-κB·DNA complex formation. A dLGG-enriched extract from *C. rabens* (10 mg/kg) markedly suppressed B16 melanoma growth in C57BL/6J mice following i.p. administration, an effect comparable with that of cisplatin, a cancer chemotherapeutic drug. This study shows the detailed molecular mechanism(s) underlying the anti-inflammatory and tumor-suppressive effects of a natural galactolipid.** [Cancer Res 2007;67(14):6907–15]

Introduction

Cancer chemoprevention concerns the use of natural or synthetic substances, alone or as a mixture, to reduce the risk of development or recurrence of cancer (1, 2). In recent years, the anticancer potential of many phytocompounds has been shown *in vitro* or *in vivo* in animal models (3): polyphenols in the leaves of tea (*Camellia sinensis*), for example, inhibits tumorigenesis and tumor growth (4, 5). The pressing need for such anticancer agents has spurred the search for phytocompounds from other sources and with novel modes of action.

Nitric oxide (NO) and its metabolite, peroxynitrite, are mutagenic because they can deaminate DNA and inactivate DNA repair enzymes (6, 7). NO is produced by the oxidative deamination of L-arginine at inflammatory sites by inducible NO synthase (iNOS), which is expressed in response to a variety of proinflammatory cytokines and bacterial lipopolysaccharide (LPS; refs. 8, 9). Improper expression of iNOS has been associated with the pathophysiology of certain human cancers and inflammatory disorders (10). Cyclooxygenase-2 (COX-2) is another important enzyme in the pathophysiology of inflammation and carcinogenesis (11, 12) through its synthesis of the precursors of prostaglandins and thromboxanes. COX-2 is expressed within human tumor neovasculature as well as in neoplastic cells in human prostate, colon, breast, and lung cancer tissues (13, 14). Because inflammation is closely linked to tumor promotion, substances with potent anti-inflammatory activities are also anticipated to have chemopreventive effects on carcinogenesis (15), especially selective inhibitors of both COX-2 and iNOS (16, 17).

Nuclear factor-κB (NF-κB), one of the principal inducible transcription factors in mammals, plays a pivotal role in inflammation through regulation of COX-2 and iNOS expression (10). NF-κB signaling involves an integrated sequence of protein-regulated steps, many of which are potential targets for inflammation and cancer treatments. NF-κB is maintained as an inactive cytoplasmic form through its association with an inhibitory molecule IκB. Exposure of cells to a variety of external stimuli, including cytokines, radiation, LPS, and reactive oxygen species, causes rapid phosphorylation of IκB, with subsequent dissociation and proteosomic degradation, allowing activated free NF-κB dimers to translocate to the nucleus (18) and induce transcription of many target genes (19). Several phytocompounds have been shown to inhibit COX-2 and iNOS expression by blocking improper NF-κB activation (20, 21). The NF-κB pathway provides exciting incentives to search for novel active phytocompounds in medicinal plants (22).

Crassocephalum rabens (Asteraceae) is a popular herbal medicine and food supplement in Taiwan for various inflammation-related syndromes. As there was no information about the truth of this reputation, we investigated *in vivo* and *in vitro* the anti-inflammatory and cancer chemopreventive properties of extracts and purified phytocompounds from *C. rabens*. We report here that a major galactolipid component, 1,2-di-*O*-α-linolenoyl-3-*O*-β-galactopyranosyl-*sn*-glycerol (dLGG), can suppress NF-κB and its downstream inflammatory mediators, NO, iNOS, COX-2, and prostaglandin E_2 (PGE_2), *in vitro*. The *in vivo* cancer prevention activity of a dLGG-rich extract from *C. rabens* was also examined against B16 melanoma growth in C57BL/6J mice.

Note: J.-H. Wu and C.-C. Huang contributed equally to this work.

Requests for reprints: Lie-Fen Shyur, Agricultural Biotechnology Research Center, Academia Sinica, Taipei 115, Taiwan, Republic of China. Phone: 886-2-26515028; Fax: 886-2-26515028; E-mail: lfshyur@ccvax.sinica.edu.tw.

doi:10.1158/0008-5472.CAN-07-0158

Materials and Methods

Cell lines and culture conditions. RAW 264.7 and B16 cells were obtained from the American Type Culture Collection. Macrophages were grown in DMEM (Life Technologies), and B16 cells were grown at 37°C in RPMI 1640 (Life Technologies), both supplemented with 10% heat-inactivated fetal bovine serum, 100 units/mL penicillin, and 100 μg/mL streptomycin, in a humidified 5% CO_2 incubator.

Materials. 3-(4,5-Dimethylthiazol-2-yl)-2,5-diphenyltetrazolium bromide (MTT), 12-*O*-tetradecanoylphorbol-13-acetate (TPA), LPS, DTT, sodium nitroferricyanide (SNP), and 2-phenyl-4,4,5,5-tetramethylimidazoline-1-oxyl-3-oxide (PTIO) were purchased from Sigma Chemical Co. Celecoxib (Celebrex) was from Pharmacia. Silica gel (230–400 mesh) and silica gel 60 F_{254} TLC and RP-18 F_{254s} TLC plates were purchased from Merck. RP-18 silica gel ($75C_{18}$-OPN) was purchased from Cosmosil. All other chemicals and solvents were of reagent or high-pressure liquid chromatography (HPLC) grade.

Animals. Female C57BL/6J mice and female ICR mice (National Laboratory Animal Center, Taipei, Taiwan) were given a standard laboratory diet and distilled water *ad libitum* and kept on a 12-h light/dark cycle at 22 ± 2°C.

Isolation and structure elucidation of dLGG. Approximately 5.0 kg of fresh whole *C. rabens* (voucher specimen CB001 in Agricultural Biotechnology Research Center, Academia Sinica, Taipei, Taiwan, Republic of China) was extracted with methanol at room temperature. Total methanol extract was partitioned with ethyl acetate to yield the ethyl acetate fraction (12.5 g), which was separated on a silica gel column with CH_2Cl_2-methanol to yield subfractions 1 to 8. Subfraction 8 was further purified on a RP-18 silica gel column eluted with 95% methanol to give a monogalactosyldiacylglycerol-enriched fraction (designated CREa8, 0.8 g). This subfraction, the most potent inhibitor of NO production in LPS-activated macrophages among the tested fractions (data not shown), was further fractionated using semipreparative RP-HPLC (Phenomenex Luna 5 μm, C_{18} column, 250 × 10 mm^2). The metabolite profile of CREa8 was characterized and the content of dLGG was determined using RP-18 HPLC. Pure dLGG (~65.7% of dry weight of CREa8) had a retention time of 12 min (100% methanol, 3.0 mL/min, $A_{205\ nm}$). ^1H and ^{13}C nuclear magnetic resonance (NMR) spectra were recorded on a Brüker ADVANCE 500 AV spectrometer.

dLGG. The characteristics of dLGG [colorless oil; electrospray-mass spectrometry (ESI-MS) *m/z* 797 $[M+Na]^+$; ^1H and ^{13}C NMR data (pyridine-d_5)] were consistent with previously published data (23). Atmospheric pressure chemical ionization/mass spectrometry (APCI/MS) was done using a Thermo Finnigan/LCQ Advantage mass spectrometer, running in positive ion mode.

Preparation of structural analogues of dLGG. dLGG in H_2O was incubated with β-galactosidase (Sigma Chemical) at 37°C for 2 days, and the product was extracted with ethyl acetate. The extract was evaporated to give 1,2-di-*O*-α-linolenoyl-*sn*-glycerol (dLG). dLG: colorless oil; ESI-MS *m/z* 635 $[M+Na]^+$; the structure of dLG was confirmed using one-dimensional and two-dimensional NMR spectroscopy.

dLGG (5 mg) was incubated with *Rhizopus arrhizus* lipase [1,800 unit/5 mL in boric acid-borax buffer (pH 7.7); Sigma] at 37°C for 30 min. The reaction was stopped by the addition of 0.1 mL acetic acid and 3 mL ethanol. The solvent was evaporated and the residue was separated by semipreparative RP-18 HPLC with 90% methanol to obtain 2-*O*-α-linolenoyl-3-*O*-β-galactopyranosyl-*sn*-glycerol (2LGG; 1.2 mg) and 1-*O*-α-linolenoyl-3-*O*-β-galactopyranosyl-*sn*-glycerol (1LGG; 0.8 mg). The characteristics of 2LGG and 1LGG [colorless oil; ESI-MS *m/z* 797 $[M+Na]^+$; ^1H and ^{13}C NMR data (pyridine-d_5)] were consistent with previously published data (23). Linolenic acid (LA) and stearic acid (SA) were from Sigma Chemical.

Measurement of NO production and cell viability. RAW 264.7 cells were treated with compound for 1 h and then incubated for 24 h with or without LPS. Nitrite levels in cell culture medium were determined using the Griess reaction (20, 24). Cell viability was examined using the MTT-based assay (25).

Determination of nitrite concentration in plasma. Female ICR mice were topically treated on their shaven back area of a 2-cm diameter (3.14 cm^2/site/mouse) with vehicle control (acetone), SNP (positive control), or with dLGG or PTIO for 30 min before SNP application. Mouse plasma samples were analyzed to determine the nitrite content following a published method (26).

COX-2 activity assays. COX-2 inhibition was measured with the chemiluminescent COX inhibitor screening assay kit (Cayman Chemical).

Measurement of PGE_2 production. PGE_2 production was determined according to the procedure of Chiang et al. (20). Macrophages were pretreated with aspirin (500 μmol/L, 3 h) to inactivate endogenous COX-1, washed, and incubated with test compounds for 1 h before further incubation for 16 h with or without LPS. PGE_2 in the culture medium was determined with ACE competitive enzyme immunoassay (Cayman Chemical).

Reporter gene constructs and luciferase assays. Four chimeric luciferase reporter genes containing either the full-length 5′ flanking promoter region (−1334/−1) or the truncations −646/−1, −320/−1, and −247/−1 bp regions of the human *COX-2* promoter were constructed in the pPGL3-Basic vector (Promega) by a published method (20). Another series of promoter constructs with specific mutations on the consensus sequences cyclic AMP–responsive element (CRE), NF-IL6, and NF-κB of full-length *COX-2* promoter were also created using PCR-based site-directed mutagenesis (27). Primer pairs for the mutations had the following sense strand sequences: CRE (−193/−187), 5′-GAAACAGTCATT*AGC*TCACATGGGCTTG-3′; NF-IL6 (−266/−258), 5′-CACCGGGCTTA*GTGC*ATTTTTTTAAGGG-3′; NF-κB (−363/−343), 5′-CAGGAGAGTG*CCC*ACTACCCCCTCTGCT-3′; and NF-κB (−587/−567), 5′-CGGGAGAG*CCC*ATTCCCTGCGCCCCCGG-3′. A double-mutated *COX-2* promoter containing mutations on both NF-κB sites was also constructed (for construct maps, see Fig. 2*A*). pPGL3-Basic vector was used as a negative control in luciferase assays. *COX-2* reporter activity in arbitrary units was normalized to that for the *Renilla* luciferase reporter.

Reverse transcription-PCR analysis. For each reverse transcription-PCR (RT-PCR) analysis, 2 μg of total RNA isolated using Trizol reagent were used to synthesize first-strand cDNA using SuperScript II Reverse Transcriptase (Invitrogen). The *iNOS* and *COX-2* genes were amplified and analyzed using specific oligonucleotide primers and PCRs by a published method (20).

Western blotting. Total cellular proteins and the specific cytosolic and nuclear proteins were prepared using methods published elsewhere (20, 21). Protein content was measured by the Bradford method (Bio-Rad). Protein was resolved by 5% to 20% gradient SDS-PAGE and subjected to immunoblotting using enhanced chemiluminescence reagents (Amersham). Monoclonal antibodies against poly(ADP-ribose) polymerase (PARP; Transduction Laboratories), glyceraldehyde-3-phosphate dehydrogenase (GAPDH; Biogenesis), α-tubulin (Oncogene Science), COX-2 (Cayman Chemical), phospho-IκBα (Ser^{32}), phospho–IκB kinase (IKK) α (Ser^{180})/IKKβ (Ser^{181}; New England Biolabs), iNOS, IκBα, IKKα/β, or NF-κB p65 (RelA; Santa Cruz Biotechnology) were used.

Immunoprecipitation and IKK kinase assay. Whole-cell lysates (300 μg) of macrophages were precleaned by incubation with 0.25 μg IgG and 20 μL protein A/G plus agarose beads (Santa Cruz Biotechnology) for 30 min at 4°C. Supernatants were then collected and incubated with IKKα/β antibody and protein A/G plus agarose beads at 4°C overnight. Precipitates were washed with immunoprecipitation buffer and kinase buffer. IKK kinase activity was assayed by adding 1 μg glutathione *S*-transferase (GST)-IκBα fusion protein (Santa Cruz Biotechnology) and 200 μmol/L ATP in 20 μL kinase buffer for 30 min at 30°C and then stopped by Laemmli's loading buffer and heated at 100°C for 5 min. Samples were subjected to immunoblotting.

Immunohistochemical study of COX-2 and nitrotyrosine protein expressions in mouse skin. Female ICR mice were topically treated on their shaven backs with vehicle (acetone), TPA, or SNP for 4 h or treated with compound (dLGG, celecoxib, or PTIO) topically for 30 min before treating with TPA or SNP for 4 h and finally killed by cervical dislocation. The formalin-fixed, paraffin-embedded skin tissues were stained according to Chiang et al. (20).

Electrophoretic mobility shift assay. Electrophoretic mobility shift assay (EMSA) was done with the LightShift Chemiluminescent EMSA kit (Pierce Biotechnology). Four micrograms of nuclear extract were incubated

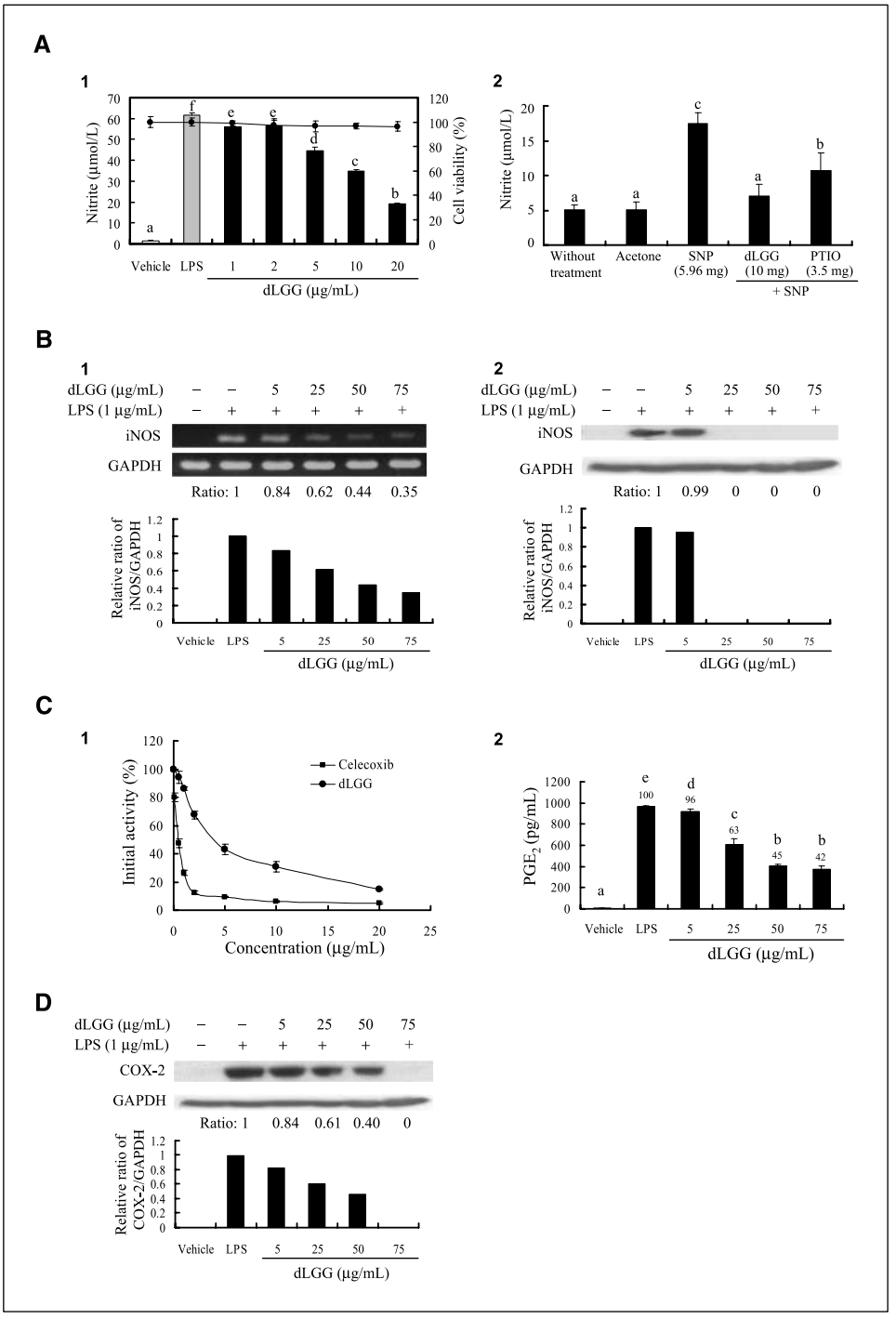

Figure 1. *A, 1,* effect of dLGG on LPS-induced NO production in RAW 264.7 cells. Cells (2×10^5 cells per well) seeded in 96-well plates were treated with or without the indicated concentrations of test compound in 0.5% DMSO (vehicle control) for 1 h, and then LPS (1 μg/mL) was added and incubated for 24 h. NO in the culture medium was measured using the Griess reagent. Survival of macrophages after treatment was measured using MTT assay and calculated by the following formula: viable cell number (%) = A_{570} (treated cell culture) / A_{570} (vehicle control) × 100. One-way ANOVA was used to analyze significance of differences. Different letters indicate significant difference ($P < 0.0001$). *2,* effect of dLGG on SNP-induced NO levels in mouse plasma. Female ICR mice were transdermally treated with 200 μL acetone (vehicle control) or SNP (5.96 mg/site) only for 15 min or pretreated with dLGG (10 mg/site) or PTIO (3.5 mg/site) for 30 min before SNP treatment. Different letters indicate significant differences among groups ($P < 0.05$). *B, 1,* effect of dLGG on LPS-induced iNOS mRNA expression in RAW 264.7 cells. Cells were treated with the indicated concentrations of dLGG for 1 h, and then LPS (1 μg/mL) was added for 6 h. Total cellular RNA was subjected to RT-PCR, and final PCR product was resolved by 1% agarose gel electrophoresis. *2,* effect of dLGG on LPS-induced iNOS protein expression in RAW 264.7 cells. Cells were treated with the indicated concentrations of dLGG for 1 h, and then LPS (1 μg/mL) was added for 18 h. Total cellular protein (20 μg) was then subjected to immunoblotting. Quantification of iNOS mRNA and protein expression involved normalization to GAPDH (internal control) by densitometry. *C* and *D,* effect of dLGG on the enzymatic activity of COX-2, PGE_2 production, and COX-2 protein expression in RAW 264.7 cells. *C, 1,* test compounds were incubated with COX-2 enzyme and substrates and measured for COX-2 activity. Celecoxib was used as a positive control. *2,* RAW 264.7 cells (1×10^4 cells per well) were treated with dLGG and then stimulated with LPS, and PGE_2 in the culture medium was then measured. Different letters indicate significant inhibition ($P < 0.05$). *D,* cells were treated with dLGG for 1 h, and then LPS (1 μg/mL) was added for 18 h. Total cellular protein (20 μg) was subjected to immunoblotting. Quantification of COX-2 mRNA and protein expression involved normalization to GAPDH by densitometry.

with biotin end-labeled NF-κB oligonucleotide, 5′-ATGTGA*GGGGACTTTCC*-*C*AGGC-3′, for 20 min at room temperature. The DNA-protein complexes were subjected to 5% to 10% gradient PAGE. Competition assay with unlabeled oligonucleotide (cold DNA) was done in parallel.

Confocal microscopy study. RAW 264.7 cells were seeded in chamber slides for 1 h and then treated with DMSO or dLGG (75 μg/mL) for 1 h, with or without LPS stimulation for an additional 90 min. Cells were fixed, permeabilized with 0.1% Triton X-100, and stained with Hoechst 33342 (DNA marker), FITC-labeled anti-α-tubulin antibody (cytoplasm marker), or rabbit anti-p65 antibody visualized with goat anti-rabbit rhodamine red–labeled secondary antibody for analysis with a Zeiss LSM 510 META confocal laser scanning microscope.

***In vivo* inhibition of tumor growth.** The chemopreventive effect of the CREa8 subfraction from *C. rabens* was evaluated on tumor growth using the B16 melanoma C57BL/6J mouse system. Six-week-old animals (four groups of five mice) were used in this experiment. Group 1 mice (Sham control) were i.p. injected with 20 μL DMSO every 2 days throughout the experimental period, except that 100 μL PBS was injected on day 0. Group 4 mice (tumor control) were pretreated with DMSO every 2 days, starting from day −14, for 2 weeks, inoculated with B16 tumor cells (1×10^6 cells/100 μL PBS) s.c. on the abdominal area on day 0, and then injected with DMSO every 2 days until day 21. Group 2 mice were i.p. pretreated with CREa8 (10 mg/kg body weight per dose) every 2 days, starting from day −14, for 2 weeks, s.c. inoculated with B16 tumor cells on day 0, and then continuously treated with CREa8 (i.p.) every 2 days until day 21. Group 3 mice were similarly pretreated with DMSO every 2 days for 2 weeks, inoculated with B16 tumor cells on day 0, and then treated with cisplatin (i.p.) every 2 days until day 21. The timeline diagram of this experimental design is shown in Fig. 6*A*. The test mice were monitored daily, and body weights and tumor size (average of two dimensions) were recorded every 2 days. At the end of the experiment (day 21), tumors were excised and weighed.

The mouse CREa8 dose (10 mg/kg body weight) in this study can be converted to a human equivalent dose (HED) based on body surface area using the following formula (Food and Drug Administration)[3]: HED = animal dose in mg/kg × (animal weight in kg/human weight in kg)$^{0.33}$, where the exponent 0.33 is used to account for the difference in body surface area between mouse and human: a dose of 10 mg/kg in a 20 g mouse converts to 0.712 mg/kg in a 60 kg human.

Statistical analysis. Data are expressed as mean ± SD. Statistical significance of differences between treatments was determined by ANOVA with Fisher's post hoc test. $P < 0.05$ was considered to be statistically significant.

Results

dLGG significantly inhibits NO production *in vitro* and *in vivo*. The inhibition of LPS-induced NO production by *C. rabens* extracts or purified dLGG was investigated in murine RAW 264.7 macrophages by determination of nitrite level (equivalent to NO level) in culture medium 24 h after treatment. dLGG significantly inhibited LPS-induced NO production in RAW 264.7 cells in a dose-dependent manner (Fig. 1*A, 1*). The IC_{50} of dLGG was ~11.4 μg/mL (14.7 μmol/L). In MTT assays, dLGG (5–20 μg/mL) did not have detectable cytotoxicity on test macrophages.

To examine the capability of dLGG to scavenge NO *in vivo*, we determined the plasma NO concentration in SNP-insulted mice with or without pretreatment with dLGG. Figure 1*A* (*2*) shows that the nitrite plasma concentration was significantly increased in SNP-treated mice compared with the vehicle-treated mice. This induced increase was suppressed by pretreatment with dLGG or PTIO, a known NO scavenger, suggesting that dLGG might be a potent NO scavenger *in vivo*.

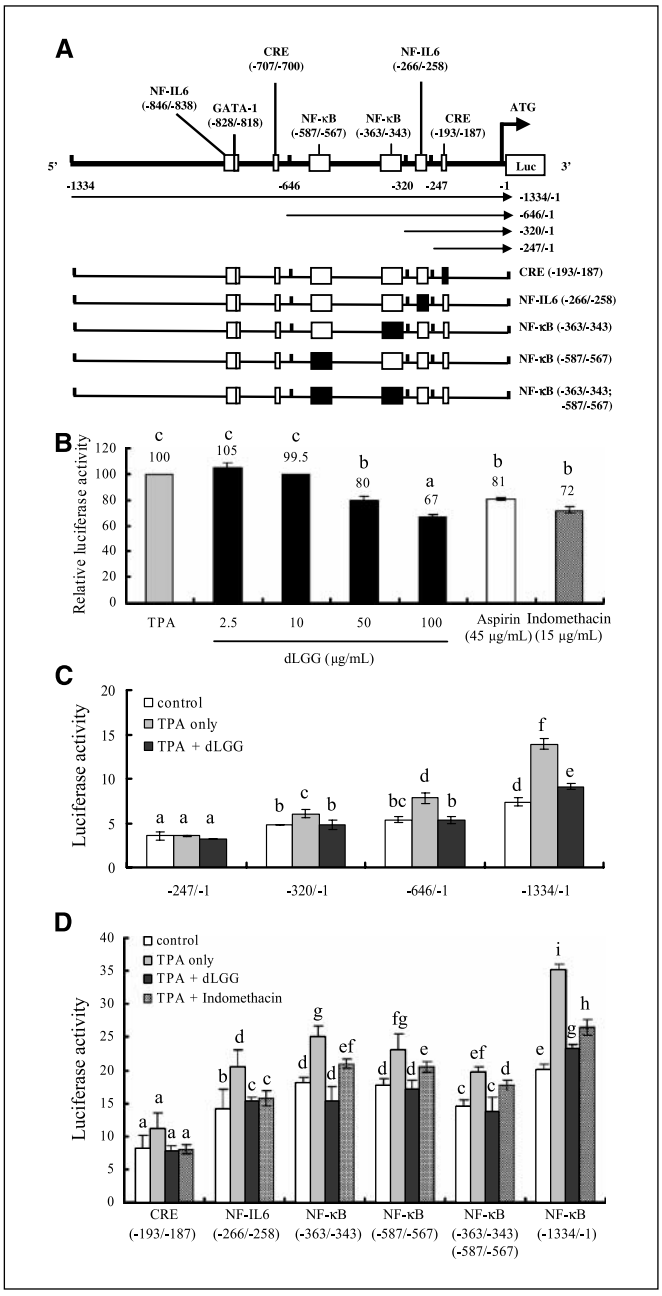

Figure 2. Characterization of the effect of dLGG on transcriptional activities of the *COX-2* promoter. *A,* map of full-length *COX-2* promoter. *Arrows,* full-length and three serial deletion *COX-2* promoter constructs. Transcription factor binding sequences in the promoter constructs with (■) or without (□) specific mutations. *B,* B16 cells cotransfected with the full-length pCOX-2-Luc and internal control *Renilla* pRL-TK-Luc plasmid constructs with the LipofectAMINE reagent (Invitrogen) were stimulated with vehicle (0.001% DMSO) or with 50 ng/mL TPA, in the absence or presence of dLGG for 6 h. Ten micrograms of total protein lysate prepared with passive lysis buffer (Promega) were subjected to dual luciferase reporter assay. The induction fold of *COX-2* promoter activity by TPA treatment only is presented as 100%. Different letters indicate significant inhibition ($P < 0.001$). *C, COX-2* promoter activities of −1334/−1, −646/−1, −320/−1, and −247/−1 constructs in control cells (*white columns*) or B16 cells treated with TPA only (*gray columns*) or TPA + dLGG (*black columns*). *D, COX-2* promoter activities of single or double mutants in vehicle control (*white columns*) or B16 cells treated with TPA only (*gray columns*), TPA + dLGG (*black columns*), or TPA + indomethacin (*sketched columns*). Data were obtained from two to three experiments with three to six replicates. *Columns,* mean; *bars,* SD. Two-way ANOVA was used to analyze significance of differences. Same letters indicate no significant difference and different letters indicate significant difference ($P < 0.01$).

[3] http://www.fda.gov/cber/gdlns/dose.htm

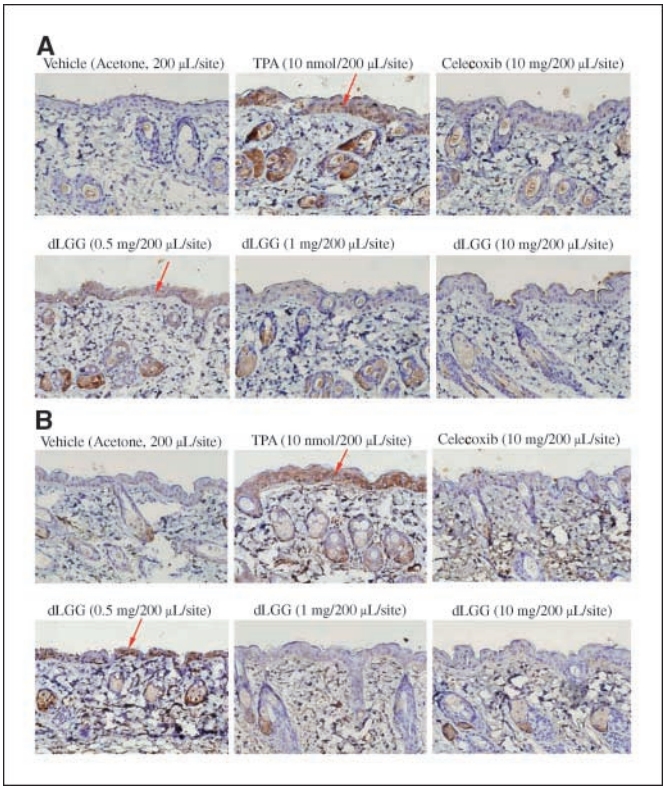

Figure 3. Immunohistochemical study of the inhibitory effect of dLGG on TPA-induced COX-2 expression and nitrotyrosine protein production in mouse skin. Dorsal skin of female ICR mice was treated topically with acetone (vehicle control) or TPA (10 nmol) for 4 h or with the indicated concentrations of dLGG or celecoxib for 30 min before TPA treatment for 4 h. Immunohistograms were taken with an Olympus DP-70 camera on a Nikon Eclipse E800 microscope. Magnification, ×200. *A,* COX-2 protein staining. *B,* nitrotyrosine protein staining. *Arrows,* positive COX-2. Nitrotyrosine staining yields a brown product.

dLGG inhibits iNOS mRNA and protein expression. The effect of dLGG on iNOS mRNA and protein expression was examined in LPS-stimulated macrophages. dLGG significantly down-regulated iNOS mRNA expression, with ~56% reduction at 50 μg/mL (Fig. 1*B, 1*), suggesting that dLGG modulates iNOS at the transcriptional level. Immunoblot also showed significant inhibition at the protein level after an 18-h treatment. Little iNOS protein was detected at 25 to 75 μg/mL dLGG (Fig. 1*B, 2*). Thus, the dLGG-induced inhibition of NO production in LPS-stimulated macrophages is also mediated through suppression of both transcription and translation of iNOS.

dLGG inhibits the enzymatic activity and protein expression of COX-2 and PGE_2 production. COX-2 activity in macrophages was significantly inhibited by dLGG, with a IC_{50} of 4.15 μg/mL (Fig. 1*C, 1*). The IC_{50} of the nonsteroidal anti-inflammatory drug celecoxib, used as a positive control, was 0.47 μg/mL. LPS-induced PGE_2 levels in macrophages were significantly reduced (37–58%) by dLGG at doses between 25 and 75 μg/mL (Fig. 1*C, 2*).

We further examined whether dLGG affects COX-2 mRNA and protein expression using RT-PCR and immunoblotting. Whereas dLGG only moderately suppressed COX-2 mRNA expression (~29% inhibition at 75 μg/mL; data not shown), COX-2 protein levels were significantly decreased in a dose-dependent manner. dLGG (50 μg/mL) suppressed LPS-induced COX-2 protein synthesis by ~60%, and at 75 μg/mL, COX-2 protein was barely detectable (Fig. 1*D*).

dLGG inhibits transcription of *COX-2*. The effect of dLGG on *COX-2* gene activity in TPA-treated B16 melanoma cells was examined. To evaluate whether important *cis*-acting elements located in the *COX-2* promoter region were affected by TPA or dLGG treatment, we constructed a series of *COX-2* promoter-luciferase reporter genes, as listed in Materials and Methods (Fig. 2*A*). TPA-induced *COX-2* promoter activity in transfected B16 cells was down-regulated by dLGG in a dose-dependent manner (Fig. 2*B*). At 50 or 100 μg/mL, dLGG suppressed full-length *COX-2* promoter activities by 20% and 33%, respectively, compared

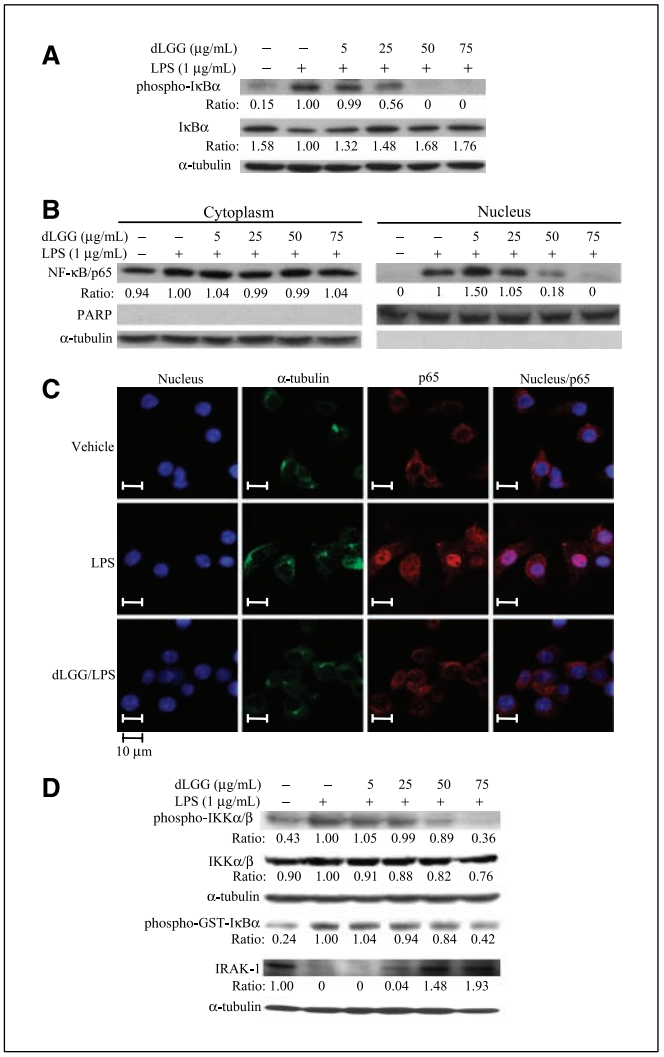

Figure 4. Effects of dLGG on IκBα phosphorylation and degradation and NF-κB translocation in RAW 264.7 cells. *A,* cells were treated with various concentrations of dLGG for 1 h followed by the addition of LPS (1 μg/mL) for 30 min. Western blots used antibodies for IκBα or phospho-IκBα. *B,* cells were treated with various concentrations of dLGG for 1 h and then stimulated with LPS (1 μg/mL) for another 90 min. Nuclear and cytosolic fractions were immunoblotted with p65 NF-κB antibody. *C,* confocal microscopy. Cells stained with Hoechst 33342 (nuclear marker; *blue*), FITC-labeled anti-α-tubulin antibody (cytosol marker; *green*), and rabbit anti-p65 (*red*). Results of one of three independent experiments. *D,* effect of dLGG on LPS-induced IKKα/β phosphorylation and IKK kinase activity and IRAK-1 degradation in RAW 264.7 cells. Cells were pretreated with various concentrations of dLGG as indicated for 1 h followed by LPS stimulation (1 μg/mL for 30 min). Specific IKKα/β and the phosphorylated forms of IKKα/β or GST-IκBα were detected by immunoblotting. IKKα/β immunoprecipitates were prepared from total cell lysate using anti-IKKα/β antibody and subsequently subjected to IKK kinase assay using GST-IκBα as substrate. PARP (nuclear protein) and α-tubulin (cytosolic protein) were used as loading controls.

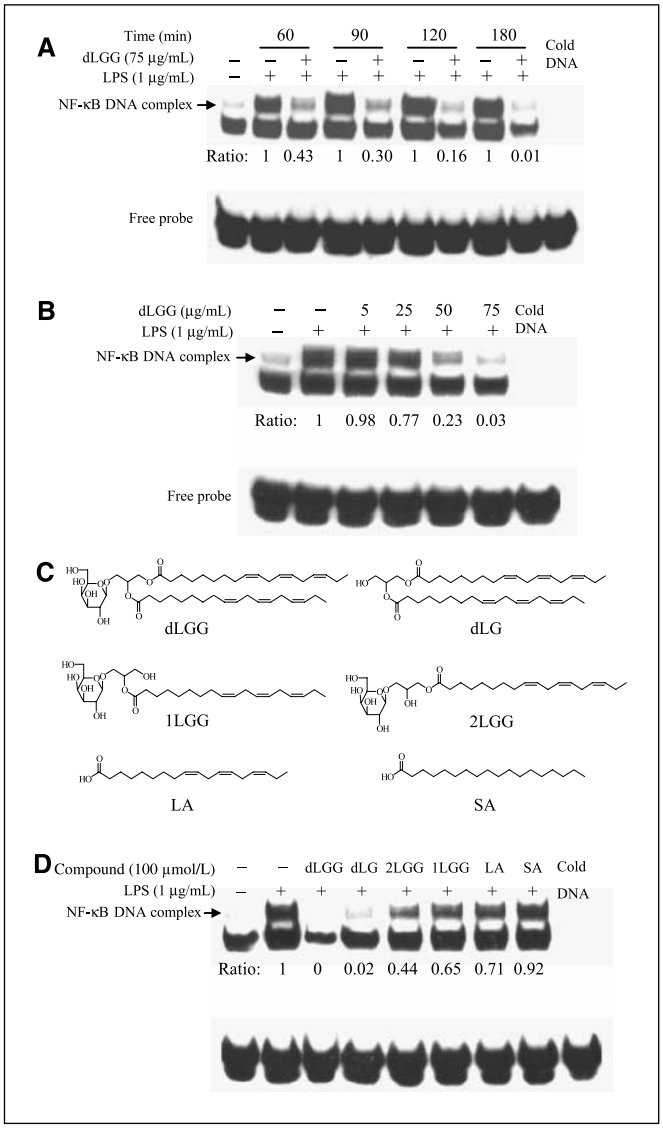

Figure 5. Inhibitory effects of dLGG on LPS-induced activation of NF-κB analyzed using EMSA. *A,* RAW 264.7 cells were preincubated in the presence or absence of dLGG (75 μg/mL) for 1 h and subsequently stimulated with LPS (1 μg/mL) for 60, 90, 120, and 180 min, respectively. *B,* cells were treated with indicated concentrations of dLGG for 1 h followed by treatment with LPS (1 μg/mL) for 90 min. Nuclear extracts (4 μg) were subjected to EMSA with a biotin-labeled DNA probe containing the NF-κB binding site. *C* and *D,* structure-activity relationship of dLGG and relative analogues using EMSA. *C,* chemical structures of dLGG and relative analogues. *D,* inhibition of LPS-induced NF-κB activation by dLGG and analogues. RAW 264.7 cells were treated with 1 μg/mL LPS and 100 μmol/L dLGG, dLG, 2LGG, 1LGG, LA, and SA, respectively, for 90 min, before EMSA. *Arrow,* gel location of NF-κB bound to DNA. Specificity of the NF-κB band was confirmed by incubation with unlabeled NF-κB oligonucleotide (cold DNA).

with cells treated with TPA only (100%). Reference controls aspirin (45 μg/mL) and indomethacin (15 μg/mL) suppressed *COX-2* promoter activity by 19% and 28%, respectively.

The full-length *COX-2* promoter was found to be highly sensitive to TPA treatment (1.9-fold increase in luciferase activity) in B16 melanoma cells (Fig. 2*C, gray columns*). Increasing promoter truncation decreased the sensitivity to TPA induction, where the −646/−1 construct showed a 1.45-fold increase in luciferase activity and the −320/−1 construct increased only 1.27-fold. The shortest construct (−247/−1) was not responsive to TPA. In the presence of 100 μg/mL dLGG, the TPA-induced luciferase activity of cells containing −1334/−1 and −646/−1 promoter constructs (Fig. 2*C, black columns*) was significantly smaller (65–68%; Fig. 2*C*). There was no difference between TPA-stimulated cells treated with dLGG (Fig. 2*C, black columns*) and the respective background luciferase activity of all transfected cells (Fig. 2*C, white columns*), showing that dLGG was able to fully inhibit any TPA-activated increases in luciferase activity.

We further examined the contribution of specific *cis*-acting element binding sites on the transcription of *COX-2* (Fig. 2*D*). TPA effectively induced *COX-2* promoter-directed luciferase activity in those constructs containing single or double mutations of the NF-IL6 or NF-κB binding sites but not the CRE mutant (Fig. 2*D, gray columns*). Importantly, dLGG was able to suppress this TPA-induced *COX-2* promoter activity in all mutant promoter constructs (Fig. 2*D, black columns*), so that luciferase activity was the same as in the respective vehicle controls (Fig. 2*D, white columns*). These results indicate that the CRE is a critical regulatory motif for TPA-induced *COX-2* transcription, whereas the CRE, NF-IL6, and NF-κB binding sites might play an equally important role in dLGG inhibition of *COX-2* promoter activity.

dLGG suppresses TPA-induced COX-2 and nitrotyrosine protein production in mouse skin. We evaluated the ability of dLGG to inhibit TPA induction of COX-2 and nitration of proteins *in vivo* using immunohistochemical analysis in a mouse skin system. After treatment with TPA (10 nmol in 200 μL/site) for 4 h, levels of COX-2 and of nitrotyrosine-containing proteins (immunostained brown) increased significantly in the epidermis, and these increases were significantly attenuated by dLGG in a dose-dependent manner. The inhibitory effect on COX-2 protein expression (Fig. 3*A*) and on nitrotyrosine-containing proteins (Fig. 3*B*) from dLGG at 1 mg in 200 μL/site (6.46 mmol/L) was comparable with that of celecoxib at 10 mg in 200 μL/site (130 mmol/L).

dLGG prevents NF-κB p65 nuclear translocation by suppressing IκBα phosphorylation and degradation. Figure 4*A* shows that the LPS-induced phosphorylation of IκBα in macrophages was inhibited by dLGG as the phospho-IκBα level decreased when the concentration of dLGG rose. The inhibition of IκBα phosphorylation also prevented IκBα degradation: IκBα continued to be detected in the presence of dLGG. The distribution of NF-κB (p65) in nucleus and cytoplasm was determined using immunoblotting. A slight increase in nuclear p65 protein (1.5-fold) was detected when macrophages were treated with a low concentration of dLGG (5 μg/mL) compared with LPS alone (1.0). With higher concentrations of dLGG (25–75 μg/mL), the level of nuclear p65 decreased accordingly (Fig. 4*B*). Cytoplasmic levels of NF-κB (p65) were not affected by dLGG treatment of LPS-stimulated macrophages (Fig. 4*B*).

The effect of dLGG on NF-κB (p65) nuclear translocation was also examined by confocal microscopy. Macrophages were treated with 0.4% DMSO or 1 μg/mL LPS with or without dLGG (75 μg/mL) and stained with fluorescence-labeled antibodies against p65 (red). To distinguish nucleus from cytosol, cells were also stained with DNA-specific Hoechst 33342 (blue) and with anti-α-tubulin antibody (green). In vehicle-treated cells, p65 protein was mainly found in the cytosol of test cells (Fig. 4*C*). After stimulation with LPS, p65 translocated from the cytosol to the nucleus, as seen in the overlapping blue and red (purple to pink) images in the column "nucleus/p65." This p65 nuclear translocation was dramatically inhibited by dLGG, as the stained p65 protein (red) remained in the cytoplasm (Fig. 4*C*).

dLGG inhibits LPS-induced degradation of interleukin-1 receptor-associated kinase-1 and IKKα/β phosphorylation and IKK kinase activity. The effects of dLGG on levels of IKKα/β and phospho-IKKα/β, the upstream kinase of IκBα in the NF-κB signaling pathway (28, 29), and the upstream kinase, interleukin-1 receptor-associated kinase-1 (IRAK-1), for activating IKK complex were examined. dLGG inhibited the LPS-induced phosphorylation of IKKα/β, whereas IKKα/β levels were little affected. In addition, dLGG inhibited IRAK-1 degradation in LPS-stimulated macrophages (Fig. 4*D*).

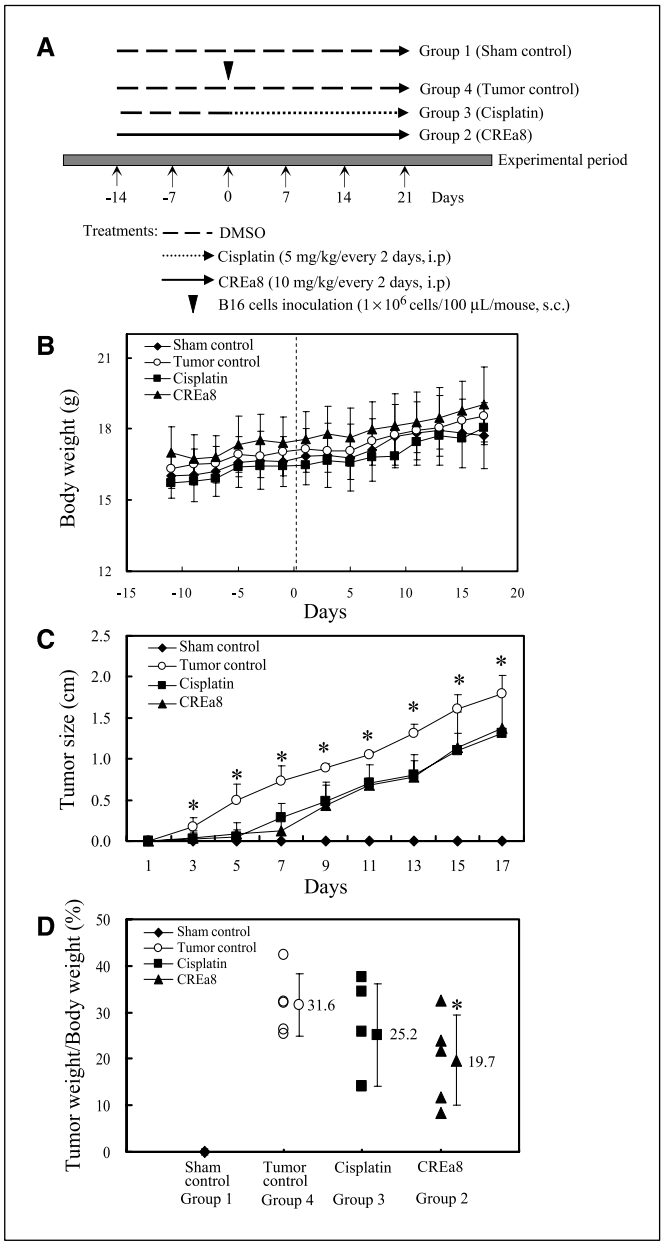

Figure 6. Effect of CREa8 (dLGG-rich fraction) on the growth of B16 melanoma tumor in C57BL/6J mice. *A,* schematic diagram of the experimental design of antitumor effect with use of a melanoma C57BL/6J mouse system. *B,* the measured body weight (g) of test mice in the four experimental groups. *C,* the measured B16 tumor sizes (cm) in the four mice groups (days 1–17). *D,* the net weight of excised tumor versus individual mouse body weight at day 21 in the four groups. ♦, group 1; ▲, group 2; ■, group 3; ○, group 4. *Points,* mean; *bars,* SD. One-way ANOVA was used to analyze significance of differences (*, $P < 0.05$).

IKK enzymatic activity was also determined to confirm whether it was correlated to the inhibition of IκBα phosphorylation by dLGG. Immunoprecipitated IKK proteins obtained from control cells (±LPS/−dLGG) or cells treated with LPS + dLGG were assayed for phosphorylation of GST-IκBα (Fig. 4*D*). The LPS-induced enzymatic phosphorylation of IκBα (phospho-IκBα) was decreased ~42% when treated with 75 μg/mL dLGG. The levels of immunoprecipitated IKK proteins were not affected by dLGG (data not shown). This result shows that dLGG abolished IκBα phosphorylation through inhibition of phosphorylation of IKKα/β and IKK kinase.

dLGG inhibits NF-κB binding to consensus DNA sequence. We observed in EMSA that stimulation of RAW 264.7 cells with LPS triggered a consensus κB DNA element binding by NF-κB (Fig. 5*A*). dLGG time dependently and dose dependently inhibited NF-κB·DNA binding activity: NF-κB·DNA complex levels with 75 μg/mL dLGG for 60, 90, 120, and 180 min were 0.43, 0.30, 0.16, and 0.01 times that of LPS alone (1.0), respectively, and 25 and 50 μg/mL dLGG for 90 min decreased NF-κB·DNA complex to 77% and 23%, respectively, of LPS alone (Fig. 5*B*). The specific binding of NF-κB to consensus DNA could be completely prevented by the addition of excess cold DNA (Fig. 5*A* and *B*).

Structure-activity relationship study of dLGG analogues. We investigated inhibition of NF-κB·DNA binding by dLGG and its structural analogues dLG, 2LGG, 1LGG, LA, and SA by EMSA. The structure of the six test compounds are shown in Fig. 5*C*. All compounds were tested at 100 μmol/L, a concentration that showed strong effects with dLGG. The inhibitory potencies were dLGG > dLG > 2LGG > 1LGG > LA > SA (Fig. 5*D*). dLGG and dLG containing dilinolenoylglycerol moieties almost completely inhibited NF-κB·DNA complex formation. 2LGG, 1LGG, and LA with only one linolenoyl chain were less effective than dLGG and dLG, whereas there was little or no detectable effect for SA. These results suggest that the linolenoylglycerol moiety is the essential galactolipid feature that hinders the formation of the NF-κB·DNA complex.

Inhibition of B16 melanoma growth in C57BL/6J mice by *C. rabens* extract. The cancer prevention efficacy of the dLGG-rich fraction (CREa8) was examined *in vivo*, using the cancer chemotherapeutic cisplatin as a reference control. The experimental strategy is presented in the schematic diagram in Fig. 6*A*. Body weights of the experimental mice in all four groups all increased gradually as a function of treatment time (Fig. 6*B*) but with no significant differences among the four groups. From 3 days after inoculation, B16 tumor growth was detected in control mice (group 4; Fig. 6*C*, ○), which grew exponentially over time (Fig. 6*C*). Test mice treated with CREa8 (group 2; Fig. 6*C*, ▲) and cisplatin (group 3; Fig. 6*C*, ■) showed a significant delay (days 3–7) and inhibition of tumor growth after B16 inoculation ($P < 0.05$). By day 7, tumors of 0.12 and 0.29 cm average size were seen in CREa8- and cisplatin-treated mice, respectively, when the tumor control mice had 0.73 cm tumors. Moreover, the average tumor sizes at day 17 in groups 2 and 3 mice were markedly reduced ($P < 0.05$), at only 76% and 73%, respectively, of the tumor control (Fig. 6*C*). For days 18 to 21, all surviving mice in the tumor control group had tumors larger than the critical size of 1.5 cm in diameter, at which point test mice were sacrificed as required by Animal Room regulations. In contrast, at the same experimental stage, three to five mice in both groups 2 and 3 had tumors <1.5 cm in diameter. Tumors were excised from all test mice on day 21. CREa8 suppressed B16 melanoma growth *in vivo* more than cisplatin (Fig. 6*D*): the tumor weight to body

weight ratio at day 21 was significantly lower in CREa8 group (19.7%; $P < 0.05$) than in cisplatin (25.2%) and tumor control (31.3%) groups. Although previous studies indicated that oral galactolipids are degraded and might not to be absorbed intact by rats (30) and are hydrolyzed by human pancreatic enzymes and duodenal contents (31), suggesting a low bioavailability of the unchanged form of dLGG and its derivatives, this study shows that i.p. administration of dLGG can significantly inhibit melanoma growth without mortality or body weight loss.

Discussion

The naturally abundant galactolipids are glycoglycerolipids with two fatty acids esterified to the glycerol *sn*-1 and *sn*-2 positions and one to four galactose units at the *sn*-3 position. Both natural and synthetic glycoglycerolipids have specific anti-algal (32), antiviral (33, 34), antitumor (35, 36), anti-inflammatory (37–40), and immunosuppressive (41) activities. However, the detailed molecular mechanisms of these bioactivities remained to be addressed. We discovered in this study that *C. rabens* plant contains a group of monogalactosyldiacylglycerols, differing in chain length and degree of unsaturation in their fatty acyl groups (e.g., C16:0, C18:1, C18:2, and C18:3), as determined by liquid chromatography-APCI/MS (data not shown). We observed that these compounds dose dependently inhibit NO production in LPS-stimulated RAW 264.7 macrophages, and the major bioactive component dLGG possesses most significant cancer chemopreventive function.

NO is an attractive therapeutic target because its overproduction has been associated with septic shock, inflammatory diseases, and diabetes. Peroxynitrite-induced protein modifications include protein oxidation or nitration of specific amino acid residues (42). Unsaturated fatty acids containing *bis*-allylic protons was suggested to undergo nitration by NO-derived species via multiple mechanisms (43) and that nitrated fatty acids are potent anti-inflammatory signaling mediators inhibiting LPS-induced secretion of proinflammatory cytokines in macrophages (44). In this light, dLGG containing two linolenic moieties may thus be a scavenger for overproduced NO. We have shown here that dLGG effectively reduced NO in LPS-stimulated macrophages and in the plasma of SNP (a NO donor)–treated mice (Fig. 1) and that dLGG also suppressed topical SNP-induced nitroprotein formation in mouse skin, with similar inhibition to PTIO, a NO scavenger (data not shown). Additionally, dLGG dose dependently inhibited iNOS mRNA and protein expression in macrophages. This is the first demonstration that a galactolipid is a potent NO scavenger *in vitro* and *in vivo*, and the reduction in NO is also partly mediated by gene and protein down-regulation of iNOS (Fig. 1).

COX-2 can foster cancer development by enhancing cellular proliferation, rendering cells resistant to apoptosis and promoting angiogenesis. The increased prostaglandin production in different types of cancers (e.g., colon, breast, and lung) is associated with increased COX-2 expression (14). In this study, inhibition of PGE_2 production by dLGG in macrophages was correlated with the attenuation of COX-2 transcriptional, translational, and enzymatic activities (Figs. 1 and 2). *COX-2* is an immediate early response gene; its expression is regulated at *cis*-acting sites by the binding of transcription factors to the *COX-2* promoter via transactivation of a regulatory signal. Our *COX-2* mutant studies reveal that although the CRE is the most important regulatory factor for TPA induction of COX-2 activity in B16 cells, CRE, NF-IL6, and NF-κB binding motifs all contributed to dLGG suppression of *COX-2* promoter activity (Fig. 2*D*). TPA-induced overexpression of COX-2 protein and protein nitration were effectively suppressed by dLGG, with an efficacy comparable with celecoxib (Fig. 3*A* and *B*). These data are the first demonstration that a galactolipid is a potent COX-2 inhibitor *in vitro* and *in vivo*.

The translocation of NF-κB to the nucleus is dependent on the phosphorylation, ubiquitination, and proteolytic degradation of IκB. The nuclear NF-κB can then transactivate several immune- or inflammatory-related genes (19). We showed that the inhibitory effect of dLGG on NF-κB nuclear translocation was due to the inhibition of LPS-induced degradation of IRAK-1 and prevention of phosphorylation and degradation of IκB through inhibition of the phosphorylation of IKKα/β and IKK kinase activities (Fig. 4). Our result shows that nuclear NF-κB DNA binding was also significantly inhibited by dLGG in LPS-stimulated macrophages. Structure-activity relationship studies revealed that galactolipids containing dilinolenoylglycerol moieties (dLGG and dLG) were the most significant inhibitors of NF-κB DNA binding. In addition, the unsaturated LA (C18:3) was more effective than SA (C18:0; Fig. 5). Similar inhibitory activity of dLGG analogues on NO production was also observed (data not shown). Therefore, we suggest that the linolenoylglycerol element of dLGG plays a critical role in preventing NF-κB transactivation and NO production in LPS-stimulated macrophages. IRAK-1 was reported to be one of the very upstream molecules activated by an adaptor protein, myeloid differentiation primary response gene 88 (MyD88), in the MyD88-dependent pathway, which leads to the translocation of NF-κB into nucleus and this in turn can regulate the expression of many genes related to proinflammatory mediators (45). We have also observed that dLGG can dose dependently suppress the binding of FITC-labeled LPS to the test macrophages (data not shown). Taken together, our results show that dLGG attenuates the activity of NF-κB and its downstream inflammatory mediators, NO, iNOS, COX-2, and PGE_2, in RAW 264.7 cells stimulated with LPS, probably due to the suppression of LPS binding to LPS receptors on the cells and the down-regulation of the MyD88-dependent pathway.

Botanical preparations have been used for treatment and prevention of various human diseases throughout history. However, as the active ingredients in plants and their mechanisms of action are usually poorly understood, scientific study of the bioefficacy and pharmacologic effects of medicinal plants is urgently needed. This report provides new insight into the molecular mechanism(s) underlying the anti-inflammatory bioactivities of a natural galactolipid dLGG from *C. rabens*. The anti-inflammatory effects of this galactolipid might be directly responsible for its significant cancer chemopreventive activity *in vivo*: the growth of B16 melanoma in C57BL/6J mice was inhibited by a galactolipid-rich fraction of *C. rabens*, with similar efficacy to current chemotherapeutic agents.

Acknowledgments

Received 1/17/2007; revised 4/20/2007; accepted 5/16/2007.

Grant support: National Science and Technology Program for Agricultural Biotechnology (NSTP.AB) grant 94S-0403 and Academia Sinica.

The costs of publication of this article were defrayed in part by the payment of page charges. This article must therefore be hereby marked *advertisement* in accordance with 18 U.S.C. Section 1734 solely to indicate this fact.

We thank High Field Nuclear Magnetic Resonance Center (National Science and Technology Program for Medical Genomics) for measurement of NMR spectra and Dr. Harry Wilson (Academia Sinica) for his careful reading of the manuscript.

References

1. Sporn MB, Suh N. Chemoprevention: an essential approach to controlling cancer. Nat Rev Cancer 2002;2:537–43.
2. Tsao AS, Kim ES, Hong WK. Chemoprevention of cancer. CA Cancer J Clin 2004;54:150–80.
3. Pezzuto JM. Plant-derived anticancer agents. Biochem Pharmacol 1997;53:121–33.
4. Lin JK, Liang YC. Cancer chemoprevention by tea polyphenols. Proc Natl Sci Counc Repub China B 2000;24:1–13.
5. Lin JK, Liang YC, Lin-Shiau SY. Cancer chemoprevention by tea polyphenols through mitotic signal transduction blockade. Biochem Pharmacol 1999;58:911–5.
6. Keefer LK, Wink DA. DNA damage and nitric oxide. Adv Exp Med Biol 1996;387:177–85.
7. Tamir S, Tannenbaum SR. The role of nitric oxide (NO.) in the carcinogenic process. Biochim Biophys Acta 1996;1288:F31–6.
8. MacMicking J, Xie QW, Nathan C. Nitric oxide and macrophage function. Annu Rev Immunol 1997;15:323–50.
9. Nathan C. Nitric oxide as a secretory product of mammalian cells. FASEB J 1992;6:3051–64.
10. Surh YJ, Chun KS, Cha HH, et al. Molecular mechanisms underlying chemopreventive activities of anti-inflammatory phytochemicals: down-regulation of COX-2 and iNOS through suppression of NF-κB activation. Mutat Res 2001;480–1:243–68.
11. Vane JR, Bakhle YS, Botting RM. Cyclooxygenases 1 and 2. Annu Rev Pharmacol Toxicol 1998;38:97–120.
12. Taketo MM. Cyclooxygenase-2 inhibitors in tumorigenesis (part II). J Natl Cancer Inst 1998;90:1609–20.
13. Masferrer JL, Leahy KM, Koki AT, et al. Antiangiogenic and antitumor activities of cyclooxygenase-2 inhibitors. Cancer Res 2000;60:1306–11.
14. Williams CS, Mann M, DuBois RN. The role of cyclooxygenases in inflammation, cancer, and development. Oncogene 1999;18:7908–16.
15. Bours V, Bonizzi G, Bentires-Alj M, et al. NF-κB activation in response to toxical and therapeutical agents: role in inflammation and cancer treatment. Toxicology 2000;153:27–38.
16. Subbaramaiah K, Dannenberg AJ. Cyclooxygenase 2: a molecular target for cancer prevention and treatment. Trends Pharmacol Sci 2003;24:96–102.
17. Cianchi F, Perna F, Masini E. iNOS/COX-2 pathway interaction: a good molecular target for cancer treatment. Curr Enzyme Inhib 2005;1:97–105.
18. DiDonato JA, Hayakawa M, Rothwarf DM, Zandi E, Karin M. A cytokine-responsive IκB kinase that activates the transcription factor NF-κB. Nature 1997;388:548–54.
19. Karin M, Lin A. NF-κB at the crossroads of life and death. Nat Immunol 2002;3:221–7.
20. Chiang YM, Lo CP, Chen YP, et al. Ethyl caffeate suppresses NF-κB activation and its downstream inflammatory mediators, iNOS, COX-2, and PGE_2 *in vitro* or in mouse skin. Br J Pharmacol 2005;146:352–63.
21. Lo AH, Liang YC, Lin-Shiau SY, Ho CT, Lin JK. Carnosol, an antioxidant in rosemary, suppresses inducible nitric oxide synthase through down-regulating nuclear factor-κB in mouse macrophages. Carcinogenesis 2002;23:983–91.
22. Bremner P, Heinrich M. Natural products as targeted modulators of the nuclear factor-κB pathway. J Pharm Pharmacol 2002;54:453–72.
23. Murakami A, Nakamura Y, Koshimizu K, Ohigashi H. Glyceroglycolipids from *Citrus hystrix*, a traditional herb in Thailand, potently inhibit the tumor-promoting activity of 12-*O*-tetradecanoylphorbol 13-acetate in mouse skin. J Agric Food Chem 1995;43:2779–83.
24. Schmidt HHHW, Kelm M. Determination of nitrite and nitrate by the Griess reaction. In: Feelisch M, Stamler JS, editors. Methods In nitric oxide research. New York: John Wiley & Sons, Inc.; 1996. p. 491–7.
25. Scudiero DA, Shoemaker RH, Paull KD, et al. Evaluation of a soluble tetrazolium/formazan assay for cell growth and drug sensitivity in culture using human and other tumor cell lines. Cancer Res 1988;48:4827–33.
26. Moshage H, Kok B, Huizenga JR, Jansen PLM. Nitrite and nitrate determinations in plasma: a critical evaluation. Clin Chem 1995;41:892–6.
27. Cheng HL, Tsai LC, Lin SS, et al. Mutagenesis of Trp^{54} and Trp^{203} residues on *Fibrobacter succinogenes* 1,3-1,4-β-D-glucanase significantly affects catalytic activities of the enzyme. Biochemistry 2002;41:8759–66.
28. Arenzana-Seisdedos F, Turpin P, Rodriguez M, et al. Nuclear localization of IκBα promotes active transport of NF-κB from the nucleus to the cytoplasm. J Cell Sci 1997;110:369–78.
29. Karin M, Ben-Neriah Y. Phosphorylation meets ubiquitination: the control of NF-κB activity. Annu Rev Immunol 2000;18:621–63.
30. Ohlsson L, Blom M, Bohllinder K, Carlsson A, Nilsson Åke. Orally fed digalatosyldiacylglycerol is degraded during absorption in intact and lymphatic duct cannulated rats. J Nutr 1998;128:239–45.
31. Andersson L, Bratt C, Arnoldsson KC, et al. Hydrolysis of galactolipids by human pancreatic lipolytic enzymes and duodenal contents. J Lipid Res 1995;36:1392–400.
32. Murakami N, Morimoto T, Imamura H, et al. Studies on glycolipids. III. Glyceroglycolipids from an axenically cultured cyanobacterium, *Phormidium tenue*. Chem Pharm Bull (Tokyo) 1991;39:2277–81.
33. Reshef V, Mizrachi E, Maretzki T, et al. New acylated sulfoglycolipids and digalactolipids and related known glycolipids from cyanobacteria with a potential to inhibit the reverse transcriptase of HIV-1. J Nat Prod 1997;60:1251–60.
34. Loya S, Reshef V, Mizrachi E, et al. The inhibition of the reverse transcriptase of HIV-1 by the natural sulfoglycolipids from cyanobacteria: contribution of different moieties to their high potency. J Nat Prod 1998;61:891–5.
35. Murakami C, Kumagai T, Hada T, et al. Effects of glycolipids from spinach on mammalian DNA polymerases. Biochem Pharmacol 2003;65:259–67.
36. Morimoto T, Nagatsu A, Murakami N, et al. Anti-tumour-promoting glyceroglycolipids from the green alga, *Chlorella vulgaris*. Phytochemistry 1995;40:1433–7.
37. Manez S, Recio MC, Gil I, et al. A glycosyl analogue of diacylglycerol and other antiinflammatory constituents from *Inula viscosa*. J Nat Prod 1999;62:601–4.
38. Berge JP, Debiton E, Dumay J, Durand P, Barthomeuf C. *In vitro* anti-inflammatory and anti-proliferative activity of sulfolipids from the red alga *Porphyridium cruentum*. J Agric Food Chem 2002;50:6227–32.
39. Larsen E, Kharazmi A, Christensen LP, Christensen SB. An antiinflammatory galactolipid from rose hip (*Rosa canina*) that inhibits chemotaxis of human peripheral blood neutrophils *in vitro*. J Nat Prod 2003;66:994–5.
40. Bruno A, Rossi C, Marcolongo G, et al. Selective *in vivo* anti-inflammatory action of the galactolipid monogalactosyldiacylglycerol. Eur J Pharmacol 2005;524:159–68.
41. Matsumoto Y, Sahara H, Fujita T, et al. An immunosuppressive effect by synthetic sulfonolipids deduced from sulfonoquinovosyl diacylglycerols of sea urchin. Transplantation 2002;74:261–7.
42. Klotz LO, Schroeder P, Sies H. Peroxynitrite signaling: receptor tyrosine kinases and activation of stress-responsive pathways. Free Radic Biol Med 2002;33:737–43.
43. O'Donnell VB, Eiserich JP, Chumley PH, et al. Nitration of unsaturated fatty acids by nitric oxide-derived reactive nitrogen species peroxynitrite, nitrous acid, nitrogen dioxide, and nitronium ion. Chem Res Toxicol 1999;12:83–92.
44. Cui T, Schopfer FJ, Zhang J, et al. Nitrated fatty acids: endogenous anti-inflammatory signaling mediators. J Biol Chem 2006;281:35686–98.
45. Bhattacharjee RN, Akira S. Toll-like receptor signaling: emerging opportunities in human diseases and medicine. Curr Immunol Rev 2005;1:81–90.